Science of the Total Environment 902 (2023) 166188

Contents lists available at ScienceDirect

Science of the Total Environment

journal homepage: www.elsevier.com/locate/scitotenv

High spatiotemporal resolution analysis on suspended sediment and microplastic transport of a lowland river

Ahmed Mohsen [a,b], Alexia Balla [a], Tímea Kiss [a,*]

[a] Department of Geoinformatics, Physical and Environmental Geography, University of Szeged, Egyetem str. 2–6, 6722 Szeged, Hungary
[b] Department of Irrigation and Hydraulics Engineering, Tanta University, Tanta, Egypt

HIGHLIGHTS

- Microplastic transport is dependent on time (hydrology) and space (source).
- Suspended sediment transport is more sensitive to hydrology than microplastic's.
- Suspended sediment and microplastic have similar sources during floods.
- Suspended sediment and microplastic transport are more independent at low stages.
- Influencing factors are event sequence, tributaries, dams and distance of sources.

GRAPHICAL ABSTRACT

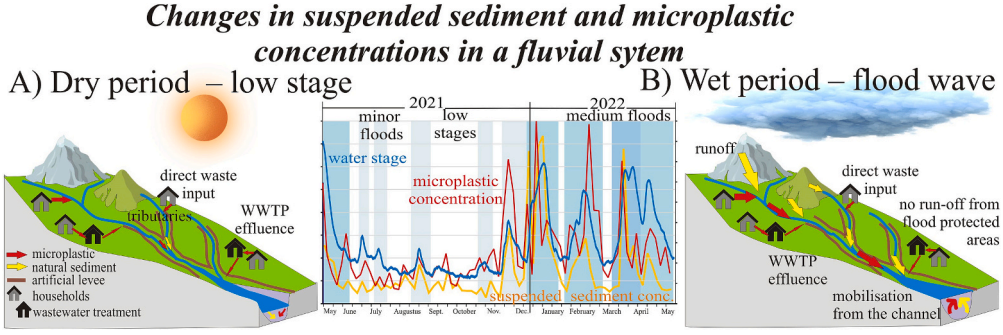

ARTICLE INFO

Editor: Damià Barceló

Keywords:
Tisza River
Temporal monitoring
Hydrology
Longitudinal changes
Tributary
Dam

ABSTRACT

The suspended sediment (SS) and microplastic (MP) transport in rivers is quite a complex process, influenced by several spatially and temporally changing factors (e.g., hydrology, sediment availability, human impact). Researchers usually investigate these factors individually and based on limited repetition in space and time. Therefore, this study aims to compare the driving factors of SS and MP transport by applying dense temporal (72 measurements) and spatial monitoring (at 26 sites). This study was performed on the medium-sized Tisza River, Central Europe. The suspended sediment concentration (SSC) was measured by water sampling and estimated based on Sentinel-2 images, while MP concentration was measured by pumping of water (1 m^3). The SSC of the Tisza varied between 12.6 and 322.5 g/m^3, whereas the MP concentration ranged 0–129 item/m^3. Most of the transported particles were fibers (81–98 %), thus, it was assumed that MPs originated from wastewater. The results reflect that the hydrological conditions basically influence the SS and MP concentrations, as a strong positive correlation was found ($\rho_{SSC-MP} = 0.6$) between them during a year; however, the correlation during floods (minor floods: $\rho = 0.63$; medium floods: $\rho = 0.41$) was higher than at low stages ($\rho = 0.1$). It was assumed that run-off and mobilization of channel materials both contribute to increased SS and MP transport during floods. In contrary, the importance of mobilization of channel materials and wastewater input increase during low stages. The repeated measurements revealed that slope and velocity conditions, proximity of sources, tributaries, and dams influence the longitudinal changes in SS and MP concentrations. However, the effects of tributaries and dams are ambiguous (especially for MP) and require further research. The longitudinal measurements were conducted at low stages; hence, moderate negative correlations ($\rho_{2021} = -0.35$; $\rho_{2022} = -0.41$)

* Corresponding author.
E-mail address: kisstimi@gmail.com (T. Kiss).

https://doi.org/10.1016/j.scitotenv.2023.166188
Received 5 June 2023; Received in revised form 7 August 2023; Accepted 8 August 2023
Available online 9 August 2023

were found between the SS and MP concentrations. Therefore, additional monitoring during (overbank) floods and denser spatial sampling are required to precisely reveal the spatiotemporal changes of SS and MP concentrations in rivers.

1. Introduction

Several studies attempted to investigate the sources, transport, and deposition of microplastics (MPs) in a fluvial environment (Zhang et al., 2020; Kiss et al., 2021); however, there are many contradicting results and unsolved questions.

Natural sediments have some similar physical characteristics with MP particles. For instance, the MP size range (0.0001–5 mm) is very similar to natural sandy and silty sediments, and both materials have various shapes and densities. They could be transported in heterogeneous aggregates with other materials as surface, suspended, or bed load, and the grains are vertically stratified according to their size and density (Cowger et al., 2021). Thus, possibly similar mechanisms govern their transport, (re-)suspension, and deposition in rivers. On the other hand, Waldschläger and Schüttrumpf (2019) reported dissimilarities between MP and natural sediment transport, as they found that half of MP particles moved earlier than anticipated by the Shields diagram, suggesting a higher MP transport rate than of the sediment. Besides, MPs usually deform during their transport and have higher fragmentation and degradation rates compared with natural sediments, complicating their transport.

Few studies investigated the correlation between suspended sediment (SS) and MP concentrations in rivers (Chen et al., 2021; Laermanns et al., 2021). In addition, they were based on measurements with limited spatial and/or temporal scales, restricting the applicability of the results, as the presented correlation may exist just at a certain spatiotemporal scale, and it is not guaranteed that it is also valid at other scales (Talbot and Chang, 2022). Moreover, contradictory results were published on the correlation between SS and MP concentrations. In particular, Chen et al. (2021) reported a significant correlation ($R^2 = 0.65$) between them, whereas Piehl et al. (2020) found no correlation. Thus, their relationship remains uncertain, and further research with finer spatiotemporal resolution is required.

Several factors, e.g., hydro-meteorological conditions, vegetation cover, and variations in sources, determine the temporal change of natural sediments and MP transport in rivers (Grove et al., 2015). However, the situation is quite complex, as during a storm, some sources might be exhausted, and/or new sources become connected to the river (Yuan et al., 2018). Seasonal variation of vegetation cover negatively relates to sediment and MP loads due to its surface stabilization effects (Talbot and Chang, 2022). The timing of mining activities, landslides, and riverbank erosion could affect the temporal variability of natural sediment without any impact on MP transport. Meanwhile, the adverse occur with variations in effluent discharges from wastewater treatment plants (WWTP) and industry (Vercruysse et al., 2017).

During floods, Ockelford et al. (2020) observed a similarity between the transport mechanism of natural sediments and MPs, as both materials followed the pattern of the hydrograph. Accordingly, the rivers are the sources/conveyors of MPs during high stages, but they act as sinks during low stages (Laermanns et al., 2021). Meanwhile, other studies (Barrows et al., 2018; Wu et al., 2020) found a negative correlation between MP transport and water discharge, considering that water discharge dilutes MPs originating from various sources.

The topography, land use, and climate of the sub-catchments and their lateral and longitudinal connectivity conditions influence the spatial distribution of natural sediments and MPs (Vercruysse et al., 2017). While the geology, mining activities, landslides, and riverbank erosion could change the spatial distribution of SS transport without any impact on the MPs, the location of WWTPs, industrial effluents (Vercruysse et al., 2017), waste management level of the sub-catchments (Mihai et al., 2022) have a contrary effect. There is a contradiction regarding the connection between MP transport and catchment features, as several studies reported a positive correlation between MP transport and urban land cover and population density (Sang et al., 2021); however, others found no correlation (Feng et al., 2020). Similarly, agricultural lands could increase MP transport due to the utilization of wastewater sludge and plastic greenhouses. However, many studies reported no correlation (Barrows et al., 2018) or even a negative correlation (Grbić et al., 2020). Tributaries could influence the spatial distribution of both materials in the main river, but they do not necessarily have the same impact in time. Dams disconnect the longitudinal transport of sediments (Serra et al., 2022), which was reported for MP too (Watkins et al., 2019).

Previous studies assessed the relationship between SS and MP concentrations based on limited repetitions in time and/or a limited number of sites; however, their relationship still needs to be clarified. Therefore, this study attempts to fill this research gap through a comprehensive spatiotemporal monitoring of SS and MP concentrations of a medium-sized transboundary river in Central Europe. This study aims to analyze the temporal changes in SS and MP concentrations through frequent measurements (every 5 days) at one site for one year and to study their longitudinal variation along the entire Tisza River (at 26 sites) in two successive years. The goals of the present study are (1) to reveal the temporal changes in SS and MP concentrations, (2) to analyze the spatial distribution of SS and MP concentrations along the Tisza River, (3) to test the persistence of identified spatial distribution patterns of both parameters at the two measured successive years, and 4) to assess the correlation between SS and MP concentrations based on the high-resolution spatiotemporal data. Thus, this study aims to determine the number of MP particles and relate it to the changing fluvial environment.

2. Study area

2.1. Geographical settings

The Tisza River is the longest tributary (962 km) of the Danube River, contributing to its discharge by 58–4346 m^3/s and draining the eastern part (157,000 km^2) of the Carpathian Basin in Central Europe (Lászlóffy, 1982) (Fig. 1). The mountainous and hilly sub-catchments are located in Ukraine, Romania, and Slovakia, whereas the lowlands are in Hungary and Serbia. The catchment is located in a moderately continental climate; thus, the annual precipitation in the mountainous sub-catchments is 1750 mm, while it is just 500–700 mm in the lowlands (ICPDR, 2018). The Tisza usually floods in early spring (March–April) due to snowmelt and early summer rainfall (June–July). Low stages occur from summer until late autumn, which is frequently associated with droughts (Kiss et al., 2008).

The Tisza was divided into three reaches (Upper, Middle, and Lower Tisza), and they were subdivided into sections (S1–S5) based on the hydrology, morphological parameters of the channel, climate, and relief characteristics of the catchment (Fig. 1).

The upstream section (S1) of the Upper Tisza's (964–688 fluvial km) is located in the Carpathian Mountains in Ukraine. It has a steep-sided, incised valley with a steep slope (20–50 m/km) and high flow velocity (2–3 m/s). The anastomosing-meandering S2 section enters the hilly (Ukraine) and lowland (Hungary) areas; thus, the channel gradually widens, and its slope decreases (from 110 cm/km to 13 cm/km). Therefore, the flow velocity drops to 1 m/s (Lászlóffy, 1982). The discharge of Tisza at Tiszabecs (site "f" at 744 fluvial km) is 14–3700

m^3/s (Q_{mean}: 207 m^3/s), and the water stage difference between the lowest and highest stages is 10.0 m (Kiss et al., 2022). The tributaries of the Upper Tisza drain water from Ukraine and Romania. Two main tributaries, the Szamos (Q_{mean}: 131 m^3/s) and Kraszna (Q_{mean}: 7 m^3/s) join the Tisza at the end of the S2 section (OVF, 2019).

The Middle Tisza (688–177 fluvial km) has a meandering pattern as the channel slope decreases (S3: ≥3 cm/km; S4: 1–3 cm/km) and the flow velocity drops (S3: ≥0.1–0.5 m/s; S4: 0.1–0.2 m/s). The mean discharge increases considerably, as, it is 509 m^3/s (range: 65–3300 m^3/s) at Szolnok (334 fluvial km), and the water stage fluctuation increases to 11.9 m (OVF, 2019). The increased discharge of the Tisza is related to the joining tributaries, namely, Bodrog (Q_{mean}: 115 m^3/s), Sajó (Q_{mean}: 27 m^3/s), Zagyva (Q_{mean}: 5 m^3/s) and Körös (Q_{mean}: 107 m^3/s) rivers (OVF, 2019). The Tiszalök and Kisköre Dams highly influence the water and sediment transport of this reach (Kiss et al., 2022). The site "u" at Mindszent (217 fluvial km) was selected for monitoring the temporal changes of SSC and MP transport for a year.

The whole reach of the Lower Tisza (177–0 fluvial km) was considered as one section (S5) since its hydro-morphological characteristics are similar (Fig. 1). This meandering/sinuous reach has the lowest slope (≤2.5 cm/km) due to the impoundment effect of the Novi Becej Dam and the Danube. The discharge at Szeged (173 fluvial km) ranges between similar values (65–4000 m^3/s) as at Szolnok, though the mean discharge (864 m^3/s) and water stage fluctuation (12.6 m) are higher than along the Middle Tisza (OVF, 2019).

2.2. Sediment transport characteristics

The bedload transport is dominant just in the mountainous Upper Tisza, as it decreases by 60 % in the lowland sections (Table 1). The SS

Table 1
Bed load and suspended sediment transport characteristics of the five sections of the Tisza River (data source: OVF, 2019).

River reach	Upper Tisza		Middle Tisza		Lower Tisza
Section (station)	S1 section	S2 (Tivadar)	S3 (Dombrád)	S4 (Szolnok)	S5 (Szeged)
Annual bed load (thousand m^3/year)	No data	22.6	8.8	11	9
Annual suspended load (million m^3/year)	No data	0.9	5	12.2	12.9
Largest suspended sed. concentration (g/m^3)	No data	3187[a]	468[b]	1200[a]	1880[a]
Mean suspended sed. concentration (g/m^3)	No data	74	85	97	384

[a] Since 1961.
[b] Since 2000.

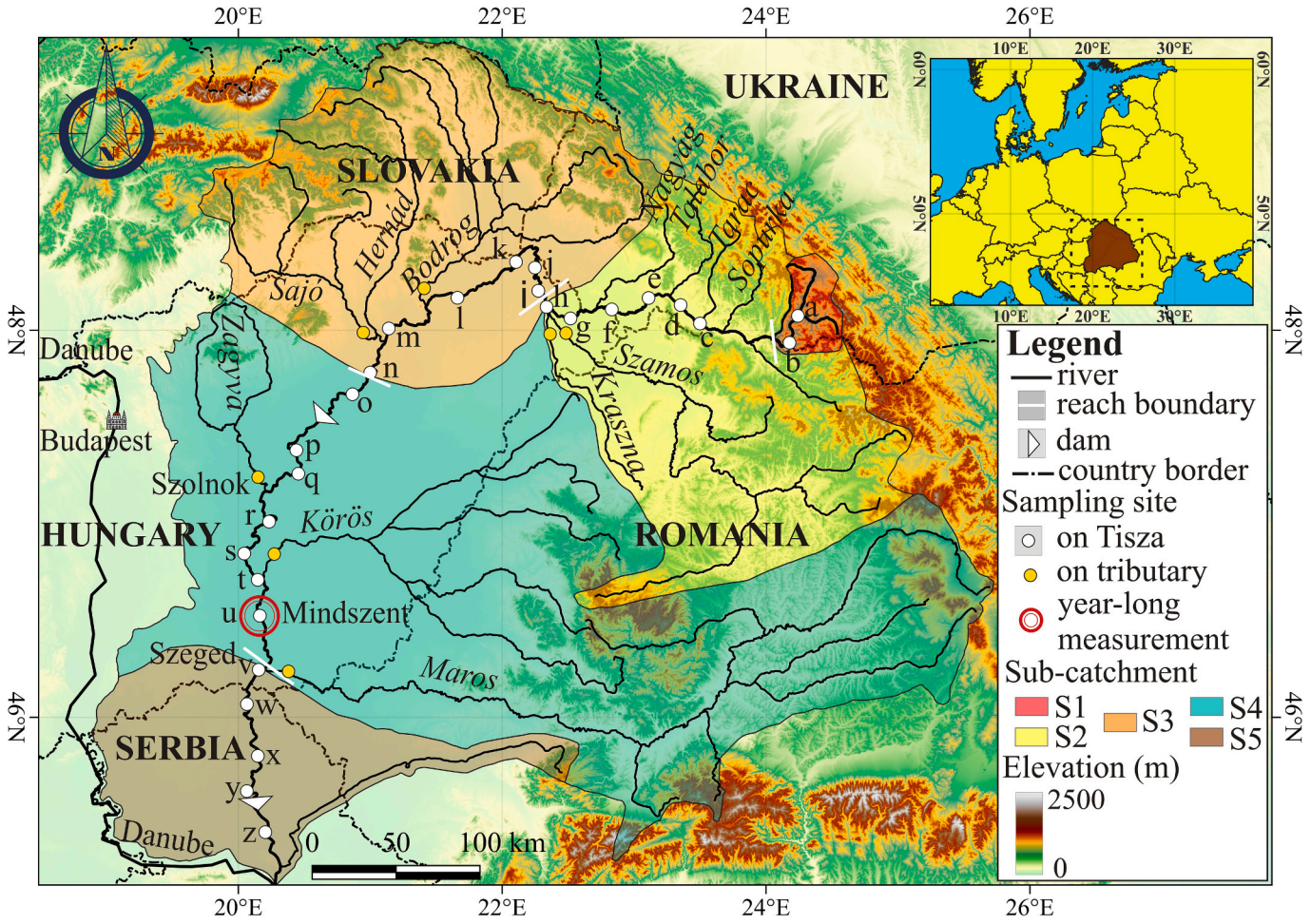

Fig. 1. The Tisza River and its catchment was divided into five sections (S1–S5) based on their hydro-morphological properties. Water samples were collected at 26 sites (a–z) in 2021 and 2022 once a year, and a 5-day frequent sampling was performed at Mindszent (site "u") for 1 year.

transport is considerable, and it increases by 14 times toward the confluence with the Danube.

The SSC is high during floods (Table 1); however, it decreases to 30 g/m^3 during low stages due to impoundment and very low flow velocity. The great temporal fluctuations are reflected by the 2001 and 2002 flood data (Csépes et al., 2000, 2003). These floods had similar hydrographs and timing (Supplement, Fig. A1), but their SS transport considerably differed, as it was ca. 50 % higher during the 2001 flood than in the 2002 flood. Usually, the SS discharge peak occurs before the water discharge peak, referring to the availability of easily erodible sediments. On the other hand, there are also considerable spatial variations in the SS transport (Supplement: Fig. A1). For instance, although similar hydrographs were recorded in 2001 and 2002 on the Middle Tisza at Kisköre (403 fluvial km) and Szolnok (334 fluvial km), the transported SS at Kisköre was on average 49 % higher than that at Szolnok, referring to overbank accumulation between them.

The tributaries also affect the sediment transport of the Tisza, especially when their high water discharge is combined with high sediment transport (OVF, 2019). In the fluvial system of the Tisza, the Maros transports the greatest amount of SS load (8.3 million t/y) with a high SS concentration (SSC_{max}: 8988 g/m^3). However, the Szamos has an even higher SSC (max: 36,461 g/m^3) followed by the Hernád (SSC_{max}: 31,229 g/m^3); however, as they have smaller water discharge, their annual contribution to the Tisza's SS transport is less (Szamos: 4.6 million t/y; Hernád 0.4 million t/y).

2.3. Plastic pollution

Compared with the Middle Tisza, the Upper and Lower Tisza reaches are more prone to pollution by mismanaged communal waste, since the waste production and recycling ratio in Ukraine and Serbia are worse than in Romania, Hungary, and Slovakia (Supplement: Fig. A2). However, the degradation of floating macroplastics is limited during the transportation process (Ronkay et al., 2021); therefore, fragments are uncommon in the microplastic load of the river (Kiss et al., 2021; Balla et al., 2022).

The most dominant MP morpho-type is fiber in the sediments and water of the Tisza (Kiss et al., 2021; Balla et al., 2022). The elevated micro-fiber abundance in the Tisza might be linked to a disparity in the ratio of houses with access to piped water and those connected to the sewage system (Kiss et al., 2021); hence, a high amount of micro-fiber is emitted to the river system from regions without sewage systems or sewage treatment. For instance, in 2011, approximately 7.8 million m^3 of untreated wastewater was drained directly into rivers in the mountainous sub-catchments of the Tisza in Ukraine (Tarpai, 2013). In Ukraine, 69 % of the wastewater is not treated, and the situation is even worse in Serbia, where 71 % is untreated. Approximately, 48 % of the collected wastewater is treated in Romania; while 98 % is treated in Hungary and Slovakia (Interreg, 2018) (Supplement: Fig. A2). On the other hand, the households that are connected to the sewage system could also increase the fiber content of the river since the other MP morpho-types are usually eliminated during the settling stage (Ngo et al., 2019). Therefore, several studies reported a higher proportion of fibers than other MP morpho-types in the effluents of WWTPs (Akyildiz et al., 2022; Koyuncuoğlu and Erden, 2023). Given that the retention ratio of the WWTPs is determined by their condition and the applied technology (primary treatment: up to 83.5 %; secondary treatment: 0–21.9 %; territory treatment: 0–12.4 %; Tang and Hadibarata, 2021), and it was reported that most of the Ukrainian WWTPs are in bad condition and mainly relied on primary or secondary treatment (Tarpai, 2013), it becomes obvious that the primary source of MP pollution in the fluvial system of the Tisza is household-related wastewater input.

3. Material and methods

3.1. In-situ data

The temporal changes in SS and MP concentrations were analyzed based on samples collected in every 5 days at Mindszent (Middle Tisza, site "u") for 1 year (May 2021–May 2022). Thus altogether, 72 samplings were performed during the year, and only two samplings (January 24 and 29, 2022) were canceled due to ice cover on the river.

The spatial changes in SS and MP concentrations were monitored during low stages in August 2021 and July 2022 along the Tisza. In 2021, samples for MPs were collected at 26 sites (a–z) along the river from its spring in Ukraine to its confluence with the Danube in Serbia; however, in 2022, the five Ukrainian sites (a–e) (Fig. 1) were skipped due to the war. The suspended sediment concentration was measured only in 2022; thus, in 2021 it was estimated by Sentinel-2 images. A detailed description of the remote sensing-based approach for SSC estimation is presented in Chapter 3.3. Additional water samples were collected in 2022 from seven tributaries (ca. 15–20 km upstream of their confluences).

We collected 1.5-L water samples for the analysis of SSC, which is representative for SSC measurement (Davis, 2005). Meanwhile, for collecting a representative sample for MP, 1 m^3 of water was pumped following Tamminga et al. (2019). The pumped water was collected from a depth of 20–30 cm and sieved through 2 metal sieves (i.e., 90 and 2000 μm). The pumping duration lasted for 25–30 min, then the residuals were washed into glass jars (350 ml). The year-long sampling (at site "u") was performed from a ferry; thus, the data represent cross-sectional averages. On the other hand, the longitudinal sampling was performed from the banks (Fig. 1).

The hydrology of the Tisza was analyzed based on daily water stage (H) data recorded at the gauging station of Mindszent, which is located 850 m upstream of the sampling site "u". The data were provided by the Hydrological Water Directorate of the Lower Tisza (ATIVIZIG).

3.2. Laboratory work

The SSC of the water samples was determined following the total evaporation method, adopting the ISO 4365 (A) and ASTM D3977-97 (A) standards (ASTM, 2007). The water was evaporated at 105 °C, the remaining sediment was weighted by an analytical balance (±0.1 mg), and the SSC was expressed as g/m^3.

The water samples for MP analysis were classified based on their SS content. Samples with high sediment content undergone through a one-step density separation process (20 ml of $ZnCl_2$ solution; 1.8 g/cm^3). The organic content of all samples was digested (cc. H_2O_2 30 %; for 48 h; Rodrigues et al., 2020; Balla et al., 2022). The samples were washed into glass Petri dishes and dried.

The MP particles were identified under a light microscope (Ash Inspex II) at 60× magnification. The visual identification of the MPs adhered to prior research criteria (Hurley et al., 2018; Balla et al., 2022). A particle was identified as plastic if (1) it had no visible cellular or organic structures, (2) the fiber had the same thickness and consistent color, and (3) it reacted with the hot needle and maintained its rigid shape when moved. Three MP morpho-types were identified, namely fiber (colored and non-colored), microbead, and fragment. The MP concentration of the water was expressed as item/m^3. To check the precision of the identification and justify the results ATR-FTIR Shimadzu Infinity 1 s device in the range from 400 to 4000 cm^{-1} was used, applying the Shimadzu Standard Library database. Altogether 150 items were selected randomly from the samples. Based on the results the precision of the identification was 98 %.

To avoid MP contamination during sampling and laboratory work, glass and metal equipment were utilized, and synthetic clothing was avoided. All tools were cleaned in an ultrasonic bath and rinsed three times with distilled water before being used, and the samples were

covered with aluminum foil. For every four samples, a fifth blank sample was prepared, which underwent the same procedure as the original samples. All the identified MP items in the blank samples were fibers (mean: 5.72 ± 3.37 items/sample); thus, the contamination increased the MP content of the samples by 8.6 % on average. Therefore, all results were corrected by extracting the number of blank MPs from the total number of a sample.

3.3. Suspended sediment concentration (SSC) estimation based on Sentinel-2 images

Since the longitudinal SSC measurements were performed solely in 2022, we relied on estimated SSC data for 2021. A machine learning-based SSC model developed by Mohsen et al. (2022) was applied to estimate the SSC at 26 sites along the river. The model was derived based on in-situ SSC measurements (2015–2020) at site "v", collected from 5 verticals of the river cross-section, and concurrent Sentinel-2 images. The reflectance of all bands, except bands 9–12, were considered as independent variables to predict SSC through several machine learning algorithms (i.e., support vector machine, random forest, and artificial neural network). The best-performing model was the combination of the three models (R^2: 0.82; RMSE: 15.43 g/m^3). However, it was reported that the model is sensitive to reflectance anomalies caused by sun glints, shadows, or waves (Overstreet and Legleiter, 2017; Mohsen et al., 2022); therefore, only clear images were used.

To estimate the SSC at a given site, 62 Sentinel-2A-B images (Level-2A) (Supplement: Table A1) were preprocessed by resampling the various bands into 10-m spatial resolution; then the Normalized Difference Water Index (McFeeters, 1996) and the OTSU automatic thresholding method (Otsu, 1979) were applied to extract the shorelines of the river. The preprocessed image was inserted into the model to estimate the SSC by averaging the concentrations of 3 × 3 pixels around the sampling point.

Since the model was developed based on in-situ SSC measurements at a particular area of the river, it is imperative to evaluate its spatio-temporal validity. Therefore, it was validated spatially by the in-situ SSC measurements covering 21 sites along the Tisza (f–z) in 2022, and temporally by the year-long SSC measurements at Mindszent ("u") site.

3.4. Data analysis

The assumptions of normality and equal variance for the spatial data of MP concentration were not fulfilled (Shapiro–Wilk normality test; $p = 0.028$), thus the nonparametric Kruskal–Wallis H and post hoc tests (Kruskal and Wallis, 1952) were applied to assess the statistical difference in MP concentration among the five sections in 2021 and 2022. The spatial distribution of the SSC followed a normal distribution (Shapiro–Wilk normality test; $p = 0.395$). Thus, the parametric one-way ANOVA test was applied to assess the statistical difference of the SSCs among the five sections.

It was hypothesized that the MP and SS concentrations depend on the hydrological conditions. Therefore, the sampling dates were classified based on the daily water stage data at the Mindszent gauging station. Low stages were identified based on their water level (H ≤ 100 cm) and limited daily water level change (≤15 cm/day), while flood waves were identified based on just daily water stage (>15 cm/day). Based on the duration, the flood waves were divided into minor (≤3 weeks) and medium floods (>3 weeks). Besides, all flood waves were subdivided into rising, peak, and falling phases. Since the temporal data of both SS and MP concentrations did not follow the normal distribution (Shapiro–Wilk normality test; SSC: $p < 0.001$; MP: $p = 0.003$), the Kruskal–Wallis H and post hoc tests were applied to reveal the statistical difference in the MP and SS concentrations among the determined hydrological periods.

Spearman's rank-order correlation test was utilized to reveal the strength of correlation between SS and MP concentrations, and water stage (ρ_{SSC-H}, ρ_{MP-H}, ρ_{SSC-MP}) during the distinguished hydrological periods (low stages: ρ_{low}; minor floods: ρ_{minor}; medium floods: ρ_{medium}; rising limb: ρ_{rising}; peak: ρ_{peak}; falling limb: $\rho_{falling}$) and along the river. The correlation was described as very strong when the correlation coefficient (ρ) was ≥0.7, strong for 0.4 ≤ ρ ≤ 0.69, moderate for 0.3 ≤ ρ ≤ 0.39, weak for 0.2 ≤ ρ ≤ 0.29 and negligible for 0.01 ≤ ρ ≤ 0.19 (Dancey and Reidy, 2007). The statistical difference was annotated by alphabetical letters in the boxplots following Mattos et al. (2017). Datasets sharing similar letters, either in a single form (e.g. "a") or double form (e.g. "ab") indicate no significant statistical difference. In contrast, datasets labeled with different letters (e.g. "a" and "b") indicate a statistically significant difference. The *p*-value for the statistically different datasets was provided too. All statistical analyses were conducted in the SPSS Statistics V 26.0 software (IBM).

4. Results

4.1. Validation of the SS concentrations estimated by Sentinel-2 images

As in 2021 we did not collect samples for SSC analysis, it was estimated by applying Sentinel-2 images and machine learning algorithms. However, it is vital to assess the validity of the applied model. Based on the water sampling at 21 sites (f–z) in July 2022 and at Mindszent "u" site for 1 year (May 2021–May 2022), a good agreement was found between the measured and the estimated SSCs, as the R^2 and RMSE were 0.87 and 16.8 g/m^3 respectively (Fig. 2). However, the SSCs were overestimated at the downstream sites (w–z) of the Lower Tisza.

4.2. Temporal changes in water level, suspended sediment and microplastic concentrations at one site within a year

4.2.1. Temporal changes in water level

A total of 72 measurements were performed between May 2021 and May 2022 at Mindszent (site "u" in Fig. 1). During this period, the water level fluctuation was 580 cm (H_{min}: −16 cm; H_{max}: 564 cm; Fig. 3). The low stages occurred during summer and autumn (H_{mean}: 21.4 ± 30 cm). They were interrupted by five minor flood waves, which were higher by 70–90 cm (H_{mean}: 92.8 ± 51.5 cm). The five medium floods (H_{mean}: 293 ± 133.5 cm) occurred in winter and spring, and they reached the bankfull level. No overbank floods (H: ≥560 cm) appeared in the studied period.

4.2.2. Temporal changes in suspended sediment and microplastic concentrations in a year

During the studied year at Mindszent, the SSC varied between 12.6

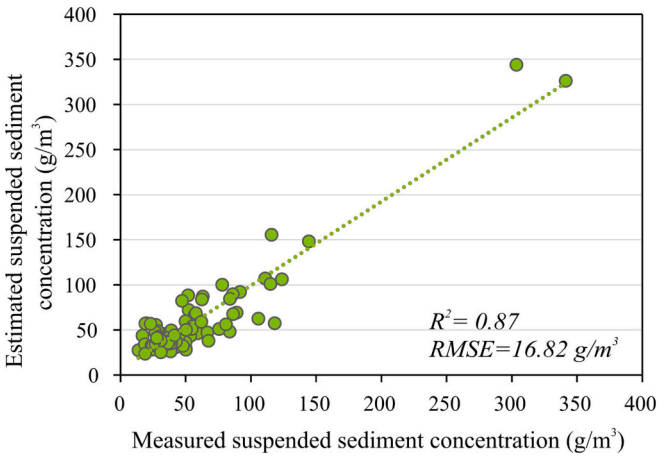

Fig. 2. Comparison of the estimated and the measured suspended sediment concentrations based on in-situ sampling of 21 sites along the Tisza (2022) and temporal monitoring at the site "u" (May 2021–May 2022).

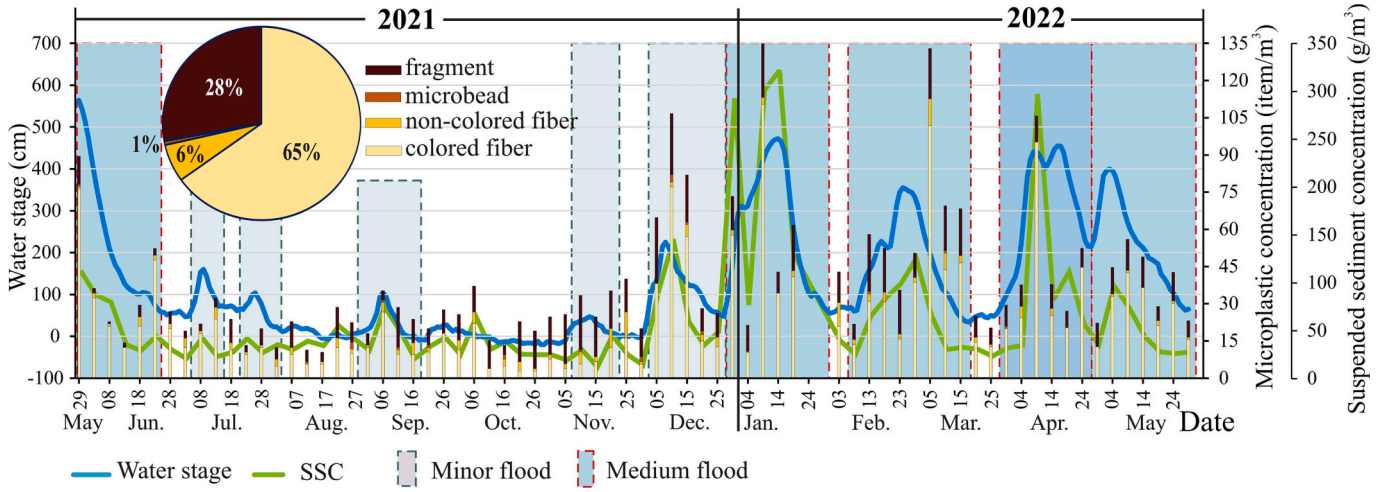

Fig. 3. Temporal changes in water level, suspended sediment (SS) and microplastic (MP) concentrations in the Middle Tisza at Mindszent (site "u") between May 2021 and May 2022.

and 322.5 g/m^3 (SSC_{mean}: 63.5 ± 65.7 g/m^3), and the MP concentration varied between 2 and 129 items/m^3 (MP_{mean}: 34 ± 26.6 items/m^3). Both the SS and MP concentrations followed the water level changes. Thus, the lowest concentrations were measured during low stages (SSC_{low}: 33 ± 1 g/m^3; MP_{low}: 18 ± 11 items/m^3), whereas the SS and MP concentrations increased by 60 % and 88.9 % respectively during minor floods. They increased further by 117 % and 41.2 % respectively, during medium floods (Fig. 4).

The mean SSCs were the same (50 ± 33 g/m^3) during the rising and falling limbs of minor floods. However, the MP concentration was lower by 12 % during their rising limb than during the falling limb (Fig. 4). Although the highest SSC was measured during the peak of minor floods (SSC_{peak}: 59 ± 16 g/m^3), it was not the case for MP concentration since it was the lowest (MP_{peak}: 20 ± 6 items/m^3). During medium floods, both SS and MP concentrations were higher during their rising limb than at the falling limb; however, the highest values were recorded concurrently with the peak of the hydrograph.

Any stagnation (e.g., January 4, 2022) or drop (e.g., April 14, 2022) in the water level during flood waves was associated with a sudden drop in the SS and MP concentrations (Fig. 3). Interestingly, the magnitude of a flood wave was not associated with similar SS and MP concentration changes. For instance, although the magnitudes of water stages of the January 2022 flood were very similar to April 2022 (considering all stages within the flood wave), the mean SSC was twice higher, and MP concentration was 1.4 higher in January than in April.

Considering all hydrological periods, the Spearman's rank correlation coefficient (ρ) was 0.71 between the SSC and water stage (ρ_{SSC-H}), and 0.61 between the MP concentration and water stage (ρ_{MP-H}) (Fig. 5A). Separating the hydrological periods, the lowest correlation occurred during low stages for both SSC (ρ_{SSC-H} = 0.31) and MP concentration (ρ_{MP-H} = 0.16), and the highest correlation occurred during medium floods (ρ_{SSC-H} = 0.78) in case of SSC, and during minor floods in case of MP concentration (ρ_{MP-H} = 0.51) (Fig. 5A, Supplement: Table A2). Considering flood phases, the SS and MP concentrations showed their highest correlation with water stage during the peak, while the lowest correlation was during the rising and falling limbs (Fig. 5B, Supplement: Table A2).

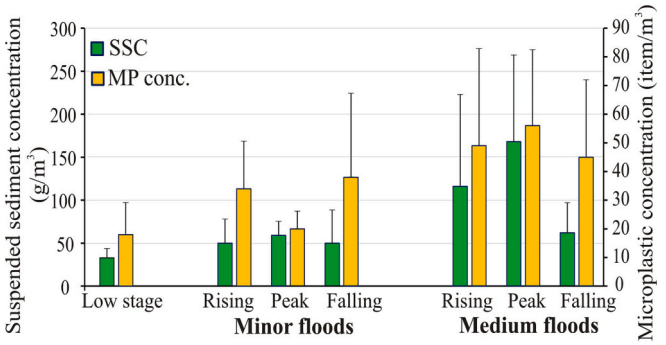

Fig. 4. Mean and standard deviation of the suspended sediment (SS) and microplastic (MP) concentrations during the distinguished hydrological periods and flood phases at Mindszent (site "u") based on a year-long measurement.

Based on the Kruskal–Wallis H and post hoc tests, a significant difference in the SSC was found only between low stages and medium floods; meanwhile, in the case of MP concentration, it was between low stages and both minor and medium flood waves (Fig. 6A, Supplement: Tables A3 and A4). Within flood waves, a significant difference occurred only between the peak and falling phases, in the case of SSC, while no statistical differences occurred between the three pairs of flood phases in the case of MP concentration (Fig. 6B, Supplement: Table A5).

Although both MP and SS concentrations were highly correlated to water stage changes during the studied year, the SSC showed higher correlation than the MP (ρ_{SSC-H} = 0.71; ρ_{MP-H} = 0.61). A strong correlation was found between MP and SS concentrations considering all hydrological periods around the year (ρ_{SSC-MP} = 0.6) (Fig. 5A). A negligible correlation was found during low stages (ρ_{low} = 0.1), while the correlation was strong during minor and medium floods, although the correlation during the minor floods (ρ_{minor} = 0.63) was higher than the medium floods (ρ_{medium} = 0.41) (Fig. 5A, Supplement: Table A2). Considering flood phases, it is interesting to note that the correlation during the falling limb ($\rho_{falling}$ = 0.45) was much lower than the rising (ρ_{rising} = 0.76) and peak (ρ_{peak} = 0.74) phases.

During the year-long measurement, most of the identified MP morpho-types were colored fibers (65 %) and fragments (27.9 %), while non-colored fibers (6.4 %) and microbeads (0.7 %) were less common (Fig. 3). The abundance of colored fibers was highly associated with medium floods (74 %), fragments, and non-colored fibers during low stages (fragments: 38 %; non-colored fibers: 12 %), and microbeads during minor flood waves (1.7 %). Considering the phases of floods, the proportion of colored fibers increased during the peak periods (79 %), while the fragments became more abundant at rising limbs (30 %) and the non-colored fibers and microbeads at falling limbs (6 % and 0.7 % respectively).

Based on the Kruskal–Wallis H and post hoc tests, only the colored fibers and microbeads showed significant differences by stage (Supplement: Fig. A3). While the colored fibers showed significant differences

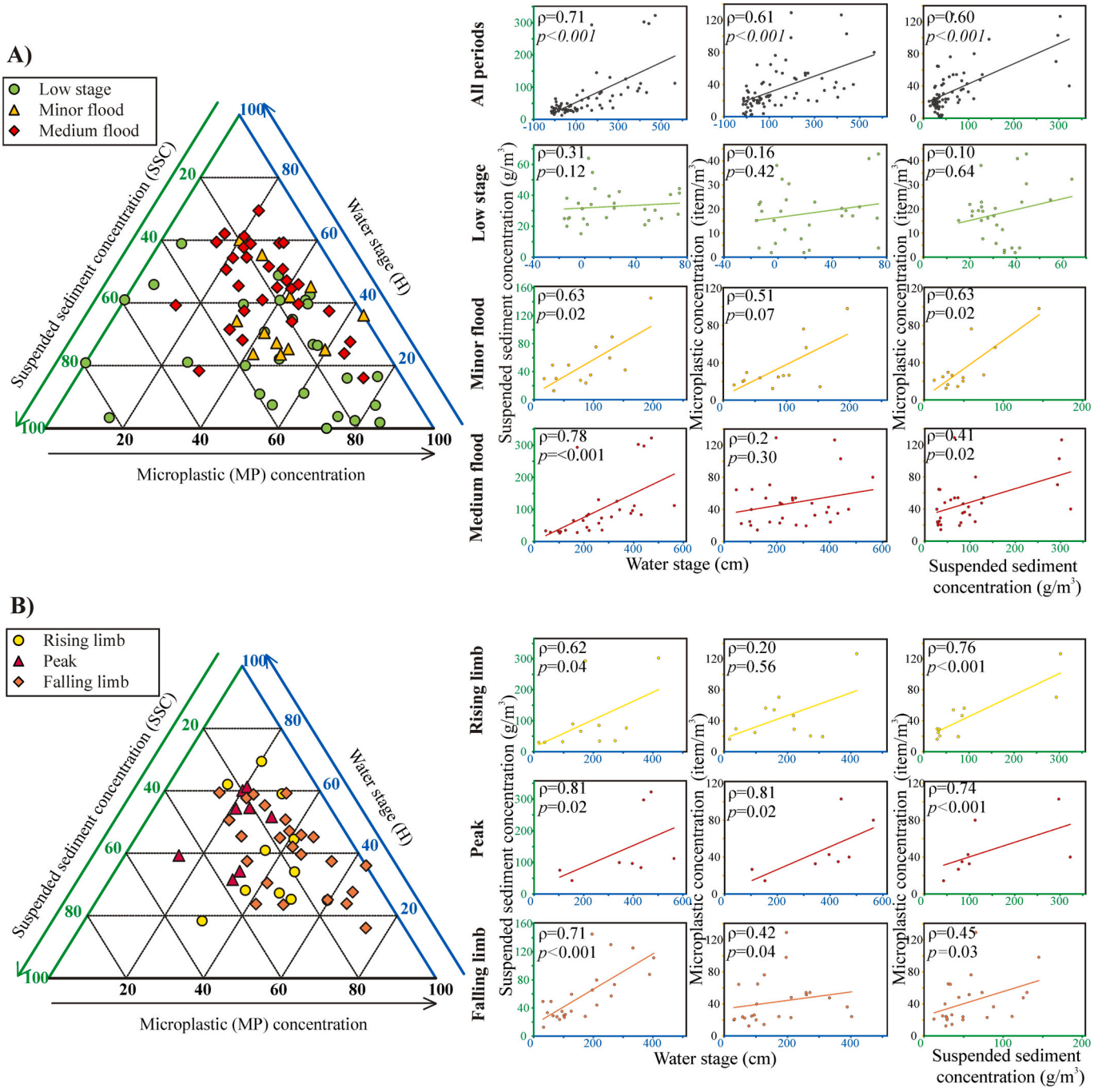

Fig. 5. Ternary plot (with normalized values) and rating curves representing the correlation between the suspended sediment (SS), microplastic (MP) concentrations and water stage (H) during the distinguished hydrological periods (A) and flood phases (B), based on the year-long measurements at Mindszent ("u") site.

among the three hydrological periods, the microbeads showed a significant difference between minor floods on one hand and both low stages and medium floods on the other hand (Supplement: Tables A6 and A7). Considering the phases of flood waves, no significant difference was found for transported MP morpho-types throughout the flood phases (Supplement: Fig. A3).

4.3. Longitudinal changes (spatial pattern) in suspended sediment and microplastic concentrations along the Tisza

4.3.1. Suspended sediment concentration of the Tisza in 2021 and 2022

The estimated SSC ranged between 26 and 44 g/m^3 (mean: 34.6 ± 4.4 g/m^3) in August 2021. The highest concentration was recorded in the S1 section, lower but similar SSCs were detected in the S2–S4 sections (Fig. 7A), and the lowest concentration was recorded in the S5 section. Based on the one-way ANOVA and Tukey post hoc tests, a significant difference in the SSC was found only between S1 and S2, S4, and S5 and between S5 and both S3 and S4 (Supplement: Table A8).

The estimated SSCs had a wider range (23.5–65 g/m^3) in July 2022 than in August 2021, and the mean concentration (40.2 ± 9.8 g/m^3) increased by 16 %. The spatial pattern of the SSC in 2022 was similar to 2021 since the highest concentrations were recorded in the S1 and S3 sections, although it increased by 38 % and 20.2 %, respectively (Fig. 7B). However, the lowest SSC was recorded in the S2 section in 2022. Based on the one-way ANOVA and Tukey post hoc tests, a significant difference occurred only between S1 and both S2 and S4

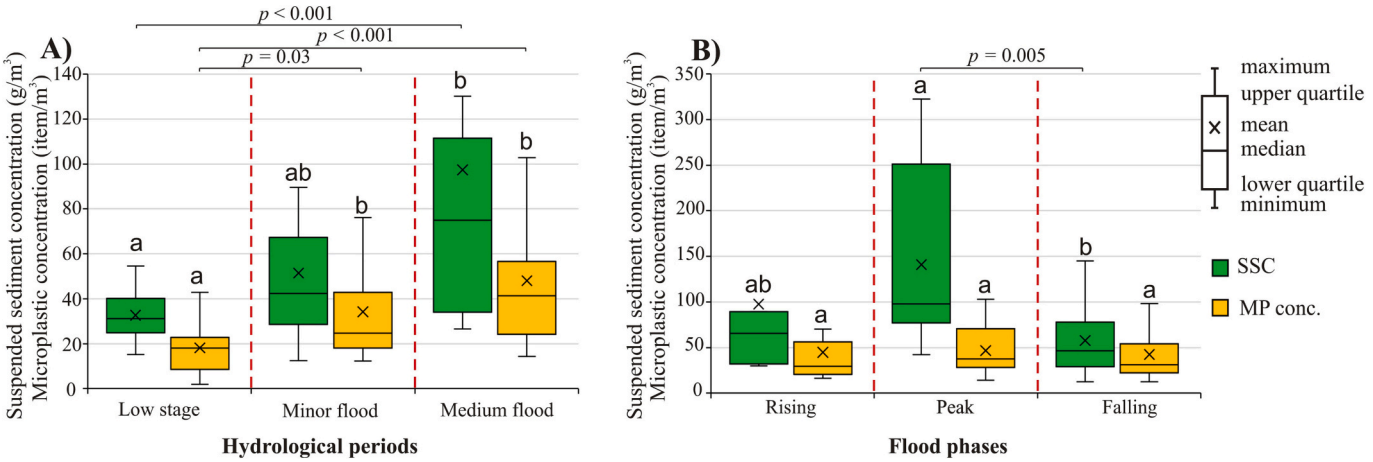

Fig. 6. Differences in suspended sediment (SS) and microplastic (MP) concentrations during the distinguished hydrological periods (A) and the flood phases (B), based on the year-long measurements at Mindszent site. Alphabetical letters indicate the statistical difference.

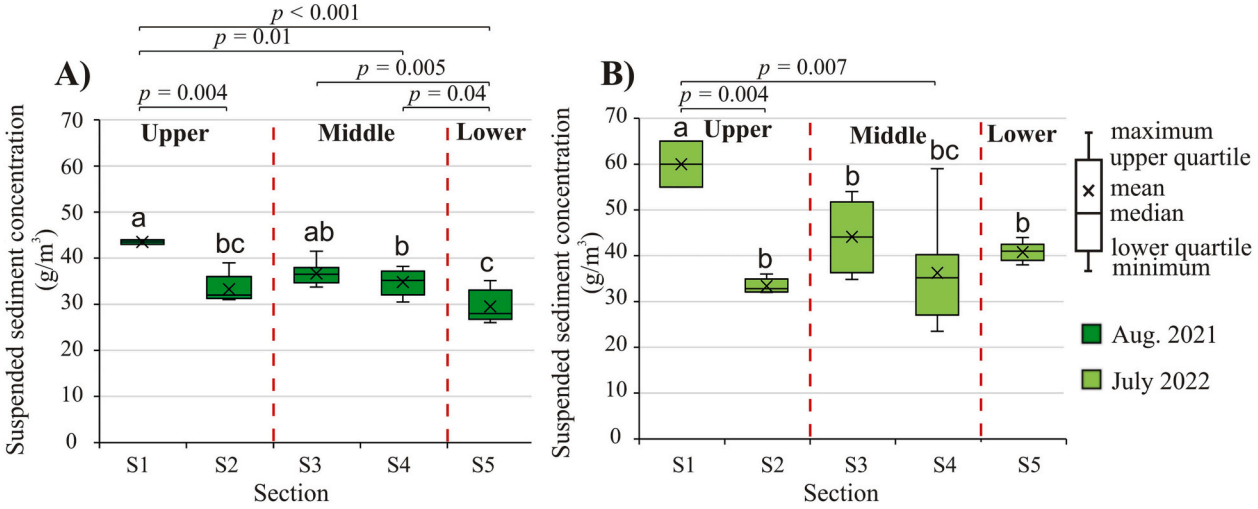

Fig. 7. Differences in the suspended sediment concentrations (SSC) among the five sections of the river (S1–5) based on the data of 26 sites estimated in 2021 (A) and 2022 (B). Alphabetical letters indicate the statistical difference.

sections (Supplement: Table A9).

The impact of tributaries on the mainstream can be evaluated by comparing the measured concentrations at sites upstream and downstream of their confluences. In 2022, the tributaries had three times more SSC (119.8 ± 59.6 g/m^3) than the Tisza (40.2 ± 9.8 g/m^3). The tributaries had diverse contributions to SSC in both years. For example, The Szamos and Kraszna increased the SSC concentration of the Tisza by 2.9–11.1 % (Fig. 8); however, downstream of the Tarac, Sajó, and Körös, the SSC declined by 15.3–27.3 %. Other tributaries (e.g., Bodrog, Zagyva, and Maros) showed an adverse effect in the two years. For example, downstream of the confluence of the Maros River, the SSC declined by 9.8 % in 2021, but it increased by 87.2 % in 2022.

Reservoirs create favorable conditions for sedimentation; however, ambiguous patterns were noticed in SSC. In the impounded upstream sections of the Kisköre and Novi Becej Dams, the SSC gradually decreased by 2.5 % and 33.5 %, respectively. However, in the most upstream Tiszalök reservoir, the SSC increased by 8.1 % and 38.5 % in both years.

4.3.2. Microplastic transport along the Tisza in 2021 and 2022

In 2021, the MP concentration ranged between 0 and 61 items/m^3 (mean: 19 ± 13.4 items/m^3). The first section (S1) was the most polluted (39 ± 31.1 items/m^3), but then the MP concentration suddenly dropped between S1 and S2 by 52.3 %, and then gradually decreased between S2 and S4 by 22 % (Fig. 9A). Finally, the MP concentration between S4 and S5 sections increased by 55.9 %. Based on the Kruskal–Wallis H test, no statistical difference in the MP concentration was found among the five sections (S1–5).

In 2022, the MP concentration fluctuated between similar values (4–63 items/m^3), although the mean (22.4 ± 14.8 items/m^3) increased by 18 % compared to 2021. The spatial pattern of MP concentration showed a similar trend in both years, since the Upper and Lower Tisza were the most polluted, and the Middle Tisza was the least contaminated (Fig. 9B). However, the MP concentration between S3 and S4 declined by 8.4 % in 2021, while it increased by 30.8 % in 2022. Similarly to the previous data, no significant statistical difference in MP concentration was found among the sections.

The section averages hide the great spatial variability of MP concentration of the Tisza between the two years (Fig. 10). In 2021, the most polluted sites were in the Upper Tisza (site "b": 61 items/m^3) and in the Middle Tisza (site "i": 42 items/m^3); however, in 2022 the most polluted site of the Upper Tisza shifted downstream to site "f" (45 items/m^3) and on the Middle Tisza to site "u" (63 items/m^3), and the site "x" (46 items/m^3) on the Lower Tisza also became very polluted. The least polluted sites in 2021 (e.g., "g" and "p") became moderately polluted in 2022, and some of the moderately polluted sites (e.g., sites "s" and "v")

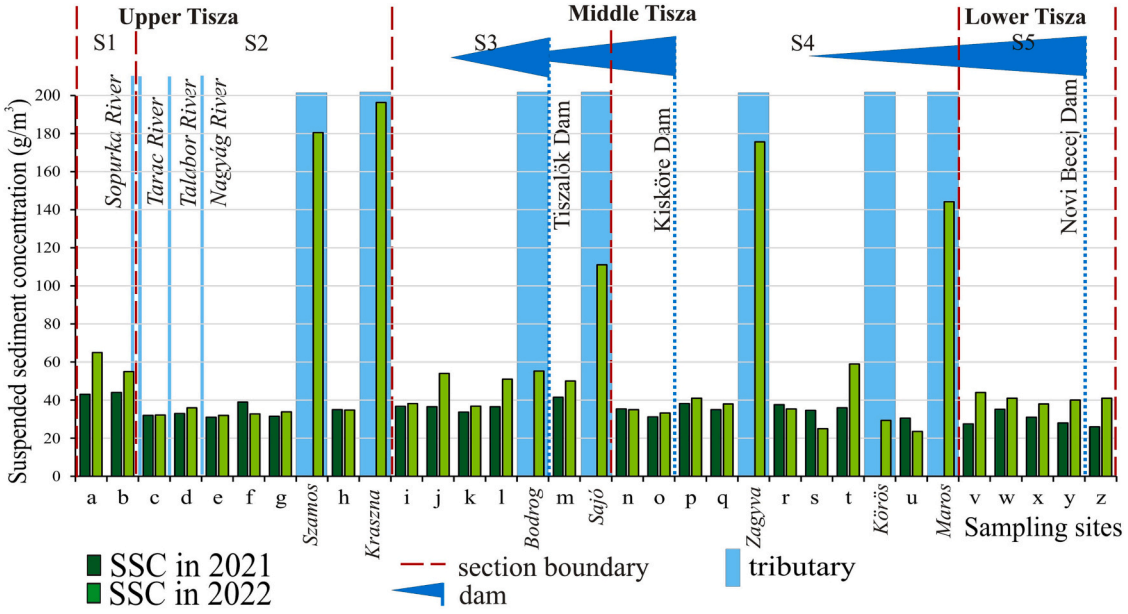

Fig. 8. Longitudinal changes in the suspended sediment concentrations (SSC) along the Tisza River at 26 sites. The July 2021 SSC data are modeled, but in August 2022 the Tisza and the main tributaries were sampled.

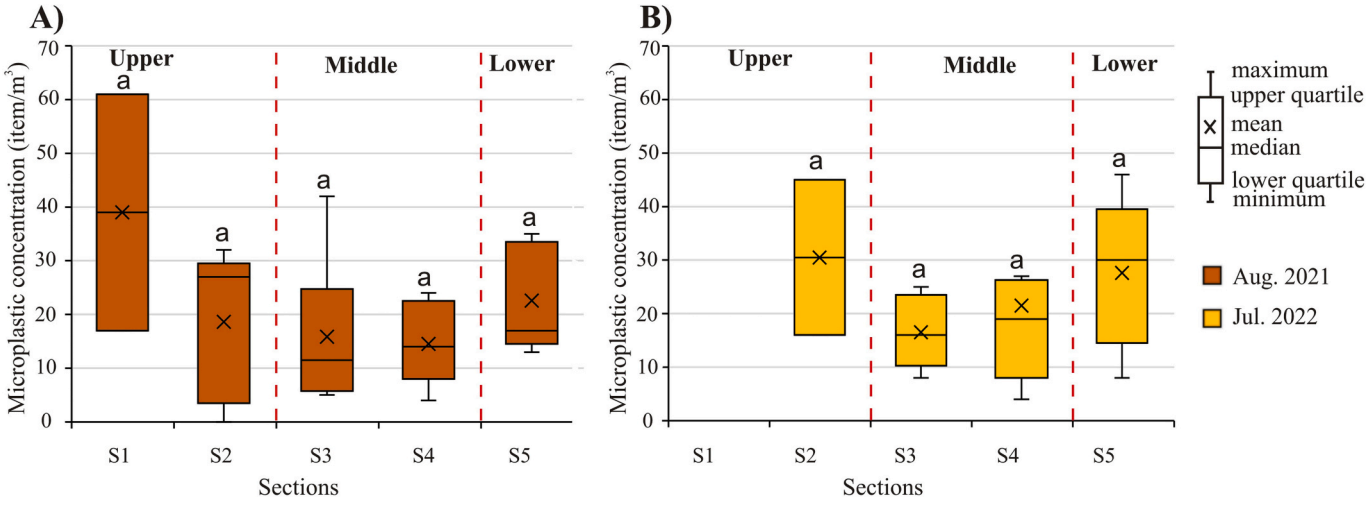

Fig. 9. Differences in the microplastic (MP) concentration among the five sections (S1–S5) based on at-a-site measurements at 26 sites (a–z) in 2021 (A) and 21 sites (f–z) in 2022 (B). Alphabetical letters indicate the statistical difference.

became less polluted.

In general, the tributaries had higher MP concentrations (27 ± 19 items/m^3) than the Tisza (22.4 ± 14.8 items/m^3). In 2021 most of the tributaries (e.g., Nagyág, Szamos, Kraszna, Bodrog, and Maros) increased the MP concentration of the Tisza by 18.5–600 % downstream of their confluences. However, in 2022, only the Kraszna and Körös increased the MP concentration by 56.3 % and 162.5 % respectively, although the transported MP by both tributaries was relatively low (11 items/m^3) compared to other tributaries e.g., Szamos (48 items/m^3) and Zagyva (63 items/m^3). In 2021, the Tarac, Sajó, and Zagyva diluted the Tisza rather than polluting it, as the MP concentration declined by 14.3–55 % as downstream of their confluences. In 2022, this diluting effect was typical downstream of the Bodrog (−27 %), and Maros rivers (−87.3 %), although in 2021, both rivers increased the MP concentration by 58.3 % and 33.3 %, respectively.

The dams ambiguously influenced the MP concentration pattern in their upstream reservoirs in both years. The MP concentration decreased by 57.9 % in the reservoir of the Kisköre Dam in 2021, but it remained the same in 2022. On the contrary, the MP concentration upstream of the Novi Becej Dam increased by 30 % (2021) and 43 % (2022).

Fibers dominated the MP pollution in both years. In 2021, most of the identified MPs were colored (44.6 %) and non-colored (39.6 %) fibers, while microbeads (8.7 %) and fragments (7.1 %) were the less common (Fig. 10). In 2022 the proportion of colored fibers (60 %) increased, the non-colored fibers (38 %) remained almost the same, and the microbeads (1.5 %) and fragments (0.4 %) became less abundant. In both years, microbeads were found just in the Middle and Lower Tisza (S3–S5), but their peaks were found at different sections. In 2021 fragments were found all along the Tisza, but in 2022, they were only in the Upper and Middle Tisza, with the highest proportion at the S2 section in both years (2021: 9.7 %; 2022: 1.6 %). Based on the Kruskal–Wallis H and post hoc tests, only the microbeads and just in 2021 were statistically different from the other morpho-types, since a significant difference was found between the S1–S3 and the S4–5 sections (Supplement: Table A10 and Fig. A4). In 2022 no significant statistical difference was found in morpho-types of the river sections.

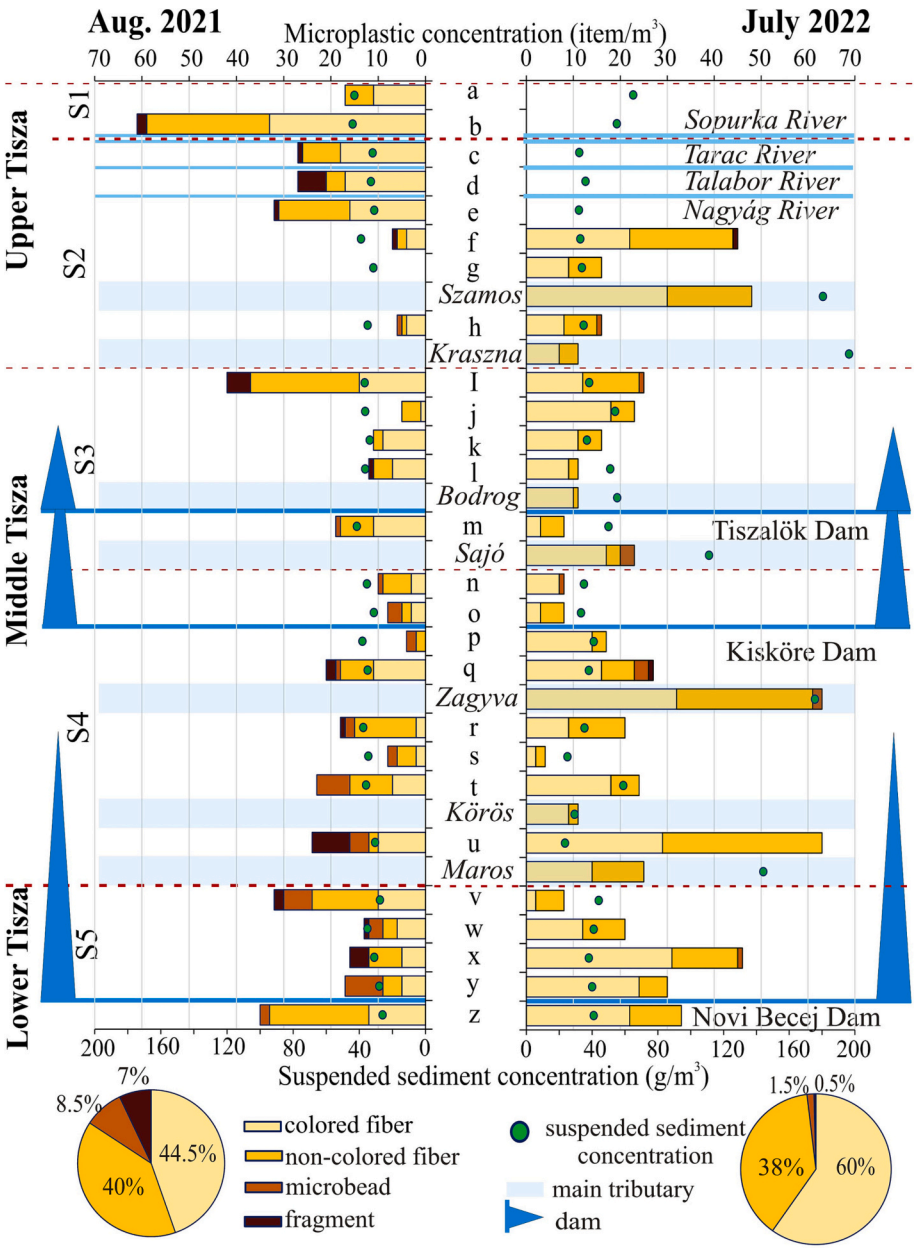

Fig. 10. Spatial distribution of the suspended sediment concentration (SSC) and microplastic (MP) morpho-types along the Tisza (at 26 sites in July 2021 and 21 sites in Aug. 2022) and the main tributaries (in Aug. 2022). The 2021 SSC data are modeled, and the 2022 ones were measured in a classical way.

4.3.3. Spatial correlation between suspended sediment and microplastic concentrations along the Tisza

Characteristic spatial patterns of the SS and MP concentrations along the river were found in 2021 and 2022 (Figs. 7 and 9). In both years, the highest SSC was measured in the uppermost (S1) and middle (S3) sections; however, the most polluted reaches with MP were found at the S2 and S5 sections. Usually, the sites with high MP pollution were associated with moderate to low SSC (e.g. at sites "e", "i", and "z" in 2021, and at sites "f" and "u" in 2022) (Fig. 10).

The tributaries influenced the SS and MP concentrations of the Tisza in 2021 and 2022 variously. Only the Kraszna (concentrating) and Zagyva (diluting) had the same impact on the SS and MP concentrations in both years, whereas the other tributaries showed temporally different impacts on the Tisza.

The SS and MP transport processes showed complex patterns in the reservoirs behind dams. The SSC showed a typical spatial trend at the low-slope Kisköre and Novi Becej Dams: it dropped upstream and slightly increased downstream of the dams. However, the MP transport displayed no similar longitudinal trend during the two surveys.

Considering all the SS and MP concentrations measurements along the Tisza River, a moderate negative correlation (ρ_{SSC-MP}: −0.35) and a strong negative correlation (ρ_{SSC-MP}: −0.41) were identified in 2021 and 2022, respectively (Table 2, Supplement: Fig. A5). Considering the river sections in 2021, the SS–MP concentration correlation ranged between moderate and very strong; however, they were positively correlated at some sections (i.e., S1 and S3) and negatively correlated at the rest of the sections. A very strong correlation between SS and MP concentrations occurred in S1 and S5 sections. A dissimilar correlation pattern was noticed in 2022, specifically for S3 and S4, which exhibited an inverse correlation sign. On the other hand, a negative correlation in the S2 strengthened in 2022 from moderate to very strong. The S5 is the only section where the correlation persisted in both years.

Table 2
Spearman's rank correlation coefficients (ρ) between suspended sediment (SS) and microplastic (MP) concentrations considering the entire river and the five sections (S1–S5) separately in 2021 and 2022.

River section		2021	2022
		SSC	SSC
Whole river (S1–S5)	MP	−0.35 ($p = 0.093$)	−0.41 ($p = 0.066$)
S1	MP	0.99 ($p < 0.001$)	–
S2	MP	−0.36 ($p = 0.553$)	−0.99 ($p < 0.001$)
S3	MP	0.64 ($p < 0.173$)	−0.10 ($p = 0.913$)
S4	MP	−0.30 ($p = 0.47$)	0.20 ($p = 0.629$)
S5	MP	−0.99 ($p < 0.001$)	−0.82 ($p < 0.089$)

5. Discussion

5.1. Comparison of the microplastic concentration of the Tisza to other rivers

The year-long measurement, which included various hydrological periods, resulted in a higher mean MPs (34 ± 26.6 items/m^3) than the longitudinal investigation along the entire Tisza at low stages (August 2021: 19 ± 13.4 items/m^3; July 2022: 22.4 ± 14.8 items/m^3). Thus, among European rivers, the Tisza could be considered as moderately polluted, as the Rhine (11.5 ± 6.3 items/m^3; Schrank et al., 2022) and the Elbe (5.57 ± 4.33 items/m^3; Scherer et al., 2020) are less polluted, while the Danube (48.7 ± 53.7 items/m^3) is more contaminated (Schrank et al., 2022). The MP concentration of the Ganges (38 ± 4 items/m^3; Napper et al., 2021) is similar to that of the Tisza; however, other Asian rivers are much more polluted (Chen et al., 2021; Yan et al., 2021). Nevertheless, the Tisza could be considered as a slightly polluted river compared to the median global MP pollution (0.17–3.4 × 10^5 items/m^3; Rodrigues et al., 2019). However, these comparisons are not entirely correct due to the lack of hydrological background and because they are constrained by the various monitoring, extraction, and identification approaches.

5.2. Possible sources of the microplastics: longitudinal and temporal variations in morpho-types

Microfiber was the dominant morpho-type (71.4 %) during the temporal measurements at Mindszent and also at all sites along the Tisza (2021: 84.6 %; 2022: 98 %), with the vast majority (44.6–65 %) being colored fibers. In the freshly deposited sediment of the Tisza, the MP particles had a similar distribution, i.e., 94–98 % of them were fibers (Kiss et al., 2021). Thus, wastewater is the major source of MP contamination of the Tisza, either by direct discharge of untreated wastewater or effluents of WWTPs (Ngo et al., 2019; Koyuncuoğlu and Erden, 2023). Similar fiber-dominated MP transport was reported in many rivers, such as the Yangtze (He et al., 2021) and the Ganges (Napper et al., 2021).

The elevated MP contamination in the Upper and Lower Tisza could be interpreted by the direct input of untreated wastewater in Ukraine, NE Hungary and Serbia, where the wastewater treatment is <30 % (Interreg, 2018), and the polluted water is discharged directly into surface waters. Besides, the wastewater in these areas is treated just by primary and secondary treatment technologies, which could retain just up to 83.5 % of the fibers (Tang and Hadibarata, 2021). Meanwhile, the moderate MP contamination of the Middle Tisza is explained by the developed wastewater management of the connecting sub-catchments.

The MPs with other than wastewater origin (e.g., runoff-related pollution) can probably get into the river system just in the mountainous sub-catchments where the waste disposal sites are not disconnected from the river. However, the contribution of runoff-related pollution is limited during low stages (Wang et al., 2022). In other areas, the MP input related to storm runoff is restricted, as the 2940 km long artificial levee system along the lowland sections of the Tisza and its tributaries acts as a buffer, disconnecting the river from its pollution sources. This hypothesis is supported by the fact that a negligible correlation exists between the MP concentration at a given site and the proportion of households connected to WWTPs along the Hungarian lowland section of the Tisza with artificial levees. A similar, loose correlation was also reported in other rivers (Tibbetts et al., 2018; Schrank et al., 2022), indicating the importance of distance and timing of the MP input, hydrodynamics, and the morphology in the transport and redistribution of MP contamination.

The concentrations of colored fibers and microbeads significantly increased during flood waves of the Tisza, being statistically different from the low stages. Thus, additional waste water sources appeared in the system during flood waves (e.g., conscious or accidental wastewater drainage).

Microbeads which usually originate from cosmetics (Bashir et al., 2021) were found just in the Middle and Lower Tisza (S3–S5). It was assumed that their less prevalence in the Upper Tisza could be connected to the low GDP of Ukraine and NE Hungary; therefore, people in these regions use less of these products.

On the contrary, fragments were the most common in the Upper Tisza (S2), where the greatest gap exists between communal waste production and recycling ratio (Eurostat, 2021). He et al. (2019) pointed out that communal waste is the major source of fragments due to the degradation of macroplastics. On the other hand, fragments may also increase at particular sites with inadequate waste management practices, or due to local anthropogenic activities (Matjašič et al., 2023). This was the case at the site of the temporal measurements (Mindszent), since fragments were also common (27.9 %), which is probably to be connected to the increased human activity in the area (i.e., fishing, tourism, ferry, and greenhouses). This distinct behavior of the selected monitoring site suggests that monitoring sites should be carefully selected and compared to understand the dynamics of various MP morpho-types in a river system.

5.3. Temporal variability of the suspended sediment and microplastic concentrations

5.3.1. In-a-year variations driven by hydrological changes at a site

Based on the year-long (72 times) measurements at Mindszent (Middle Tisza), it became clear that the SS and MP concentrations are closely related to each other ($\rho_{SSC-MP} = 0.6$) and to hydrologic changes. However, MP concentration to water stages has a lower correlation than the SSC (ρ_{MP-H}: 0.61; ρ_{SSC-H}: 0.71), indicating that the MP transport is less dependent on hydrological conditions than the SS transport. Several studies reported such a positive correlation (Ockelford et al., 2020; Laermanns et al., 2021), although others described a negative correlation (Barrows et al., 2018; Wu et al., 2020). However, no evidence on this negative correlation was found in the Tisza during the year.

The SS and MP concentrations decreased during low stages, when the flow velocity dropped (≤0.02 m/s), and the low transport capacity stimulated the deposition of both SS and MP particles. However, during low stages, the MP and SS concentrations showed a negligible correlation with each other and were weak with the water stage. Chen et al. (2021) explained the lower correlation during low stages by the existence of non-flood related sources (e.g., bank erosion, wastewater input), whereas the dominance of storm runoff and resuspension of bottom sediments increased the transport of the particles during higher stages.

During small flood waves, the increased flow velocity (>0.25 m/s) and the turbulent flow mobilized the deposited sediments and MP from

the bottom of the channel. Thus, the strongest correlations were found between MP concentration and SSC ($\rho_{SSC–MP}$: 0.63) and water stage ($\rho_{MP–H}$: 0.51) during minor floods, indicating that the mobilization of channel-bed sediments has a similar effect on SS and MP transport, and that both variables are sensitive to stage changes.

In case of medium flood waves, the situation became more complex, since they are generated by runoff in the upper sub-catchments. Thus, not only the in-channel sediments but also the slope sediments are mobilized, including MP sources (Karimaee Tabarestani and Zarrati, 2015). Therefore, the correlation between MP and SSC ($\rho_{SSC–MP}$: 0.41) and water stage ($\rho_{MP–H}$: 0.2) declined. This suggests that surface run-off has dissimilar impacts on MP and SS transports, due to their heterogeneous availability within the sub-catchment. This idea is also supported by the differences in SS and MP concentrations and flow velocity changes within the phases of the medium flood waves, as the sediment and MP transport was higher in their rising limbs than in the falling limbs, referring to greater availability of sediments in the channel and on the slopes in the upland sub-catchments at the beginning of a flood (Talbot and Chang, 2022).

Considering all floods, the correlations between the SS and MP concentrations during their rising limb and peak phases were very strong ($\rho_{rising} = 0.76$; $\rho_{peak} = 0.74$), while a moderate correlation occurred during the falling limb ($\rho_{falling} = 0.45$). Probably the kinetic energy attenuated exponentially at the falling limb, and the thickness of the active layer of the bottom sediments decreased and stabilized (Ockelford et al., 2020). Therefore, the flood-related sources/factors of the SS and MP transport (e.g., storm runoff and resuspension of deposited materials) diminished and substituted by low stage sources/factors (e.g., tributaries and WWTPs), which have different impacts on the SS and MP transport.

Evidence of the first flush effect was noticed in the Tisza after a low stage period. The first flood wave had twice higher SSC and 1.4 times higher MP concentration than the subsequent flood waves. Furthermore, the sediment and MP transport was higher in the rising limbs than in the falling limbs of flood waves. These observations refer to the greater availability of sediment and MP in the channel and on the slopes in the upland sub-catchments at the beginning of a flood (Talbot and Chang, 2022). During floods, the SSC peak usually occurs concurrently with the flood peak, while the maximum of MP concentration could precede or follow it (Fig. 3). This lag of the MP concentration peak could be explained by the different transport lengths of the materials (Ockelford et al., 2020; Chen et al., 2021) or by the earlier mobilization of light MPs (Waldschläger and Schüttrumpf, 2019). The importance of event sequence was also reported by Vercruysse et al. (2017), which should get more emphasis during the assessment of MP pollution data.

5.3.2. Variations between two years along the river

The longitudinal measurements were performed at low stages with low SSCs. The mean SSC of the Tisza in 2022 was 16 % higher than in 2021, and the MP concentration was also higher by 18 %, though the water stage in 2022 (−20 cm) was lower than in 2021 (9 cm). This difference can be explained by the fact that the 2022 sampling campaign was conducted in July after heavy rainfalls on the sub-catchments and the onset of the tourist season when motorboats and jet skis stirred up the water. On the other hand, the 2021 sampling campaign was made at the end of the low stage period in late August when the tourist season terminated, and the lack of disturbances stimulated the in-channel deposition of SS and MP. Therefore, it is suggested to perform SS and MP concentration monitoring in identical, eventless hydrological periods.

5.4. Spatial variability of the suspended sediment and microplastic concentrations

On the section scale, the spatial pattern of SS and MP concentration in 2021 was similar to 2022. However, the mean and median values increased in 2022, referring to increased SS and MP transport into and within the river system. Only a moderate negative correlation between the SS and MP concentrations was found (2021: $\rho_{SSC–MP}$: −0.35; 2022: $\rho_{SSC–MP}$: −0.41), although it had a positive correlation at some sections (e.g., S1). The moderate correlation is related to the timing of the measurements, as they were performed at summer low stages. Moreover, as the year-long measurements at Mindszent suggest, the correlation between SS and MP concentrations is negligible ($\rho_{low} = 0.1$) at low stages.

Our spatial measurements were conducted during low stages; thus, the interpretations might be limited to this period. It is essential to undertake additional measurements during floods to verify the validity of such interpretations under other hydrological conditions. However, it is quite challenging to collect samples during floods in a large fluvial system, as (1) flood waves can travel at different speeds and the sampling lasts almost for a week; thus, it is difficult to collect samples from always the peak of the flood at every site; (2) some tributaries might contribute to floods while others not, so that the flood wave could appear just in certain sections of the main river.

5.4.1. Longitudinal variability and distance from pollution sources

The mountainous section (S1) of the Upper Tisza is the only one where the SS and MP concentrations were strongly and positively correlated ($\rho_{SSC–MP}$: 0.99) since the highest SSC (43.5 ± 0.5 g/m^3) was associated with the highest MP concentration (39 ± 22 items/m^3). Since the S1 section is located in a mountainous sub-catchment with no artificial levees, heavy rains could generate rapid runoff that mobilizes the slope sediments and wastewater storages. Thus, the transport of SS ad MP was strongly related due to the connectivity of the river to sediment and MP sources. Toward the S2 section, the slope decreases, and a floodplain appears in the valley. Simultaneously, the population increases, but it accompanied with poor wastewater treatment in Ukraine and NE Hungary, increasing the amount of (untreated) wastewater input. The combination of these natural and anthropogenic factors results in decreasing SSC and increasing MP concentration. Thus, a moderate negative correlation ($\rho_{SSC–MP}$: −0.36) was found in 2021, which became a very strong negative correlation ($\rho_{SSC–MP}$: −0.99) in 2022.

The SSC increased in the Middle Tisza (S3–S4) because several large tributaries with considerable SS transport join the Tisza. Béjar et al. (2018) reported similar results, as the SSC increased by fourfold at a reach with several tributaries. However, the MP concentration decreased compared to the Upper Tisza, as the wastewater management in this region is very good (the proportion of households connected to wastewater systems is over 77 %); thus, the correlation between the two parameters became weaker (in 2022 S3: $\rho_{SSC–MP}$: −0.1; S4: $\rho_{SSC–MP}$: 0.2).

Finally, a very strong negative correlation (2021: $\rho_{SSC–MP}$: −0.99; 2022: $\rho_{SSC–MP}$: −0.82) was found in the Lower Tisza (S5) in both years. Here the impoundment by the Novi Becej Dam declined the SSC by supporting sediment deposition upstream of the dam; however, the low-degree wastewater management in Serbia increased the MP contamination. Although correlations between SS and MP concentrations were established at a section scale, further research is required by applying more sampling sites.

There was high variability in SS and MP concentrations at a site scale. The SSCs were especially varied in 2022, probably because the sampling was performed in July when minor flood waves could locally increase the sediment transport (see sites along S1). The locations of the most and least polluted MP sites also changed. Flow changes, variations in pollution sources, changes in local human activities, and alterations in waste management practices could explain this great spatiotemporal variability. Also, it suggests that the MP pollution is transported in waves (similarly to SSs), but it is not necessarily related to real flood waves, as the longitudinal measurements were made at low stages. It suggests that much denser spatio-temporal sampling should be applied to understand the MP transport and deposition.

5.4.2. Effect of slope on transport processes

The MP transport had no clear downstream trend along the 962 km length of the Tisza, as the highest MP concentrations were recorded in the Upper Tisza with high water slope (>13 cm/km) and in the Lower Tisza with almost no slope (≤2.5 cm/km). Meanwhile, the Middle Tisza (1–3 cm/km) was the least contaminated. This contamination pattern indicates that the influence of slope conditions on MP transport is outweighed by other factors (e.g., anthropogenic activities, runoff patterns, and sediment deposition). Therefore, if sampling is performed along longer reaches, the longitudinal trend in MP transport could be disrupted (Schrank et al., 2022). Our assessment is based on low-stage measurements when the river has the lowest slope (Kiss et al., 2019); thus, the slope likely has minimal impact on SS and MP transport. In the meantime, the influence of slope conditions may change during floods; hence further longitudinal measurement during floods is warranted for comprehensive evaluation.

5.4.3. Effect of tributaries on transport processes

Tributaries play a significant role in SS and MP transport of the mainstream, though their effect on SS transport is more evident than MP's. Temporal variations in MP and SS transport of the studied tributaries and differences in their impact on the Tisza were revealed, similar to the results of Béjar et al. (2018) and Mouri et al. (2014). Although tributaries had three times higher SSC than the Tisza (in 2022), especially in the Middle Tisza with the major tributaries, they influence the SSC and MP concentration of the main river only slightly, because of their low discharge, especially during low stages. However, more data is needed to understand their role in SS and MP transport of the main stream, as the discharge ratio of the tributary and the main river, the mixing patterns, and the propagation of flood waves could influence the snapshot-like results.

5.4.4. Effect of dams and reservoirs

Dams affect the longitudinal SS transport partly by supporting sediment deposition in their impounded upstream sections; and by increasing it downstream of the dams as the clear water erosion mobilizes the channel-bottom sediments (Kondolf et al., 2014; Chen et al., 2021). However, the revealed SS and MP transport patterns were contradictory in the reservoirs of the Tisza in 2021 and 2022, though the SS transport showed a more consistent pattern. This variability might be attributed to the relatively uniform characteristics and settling behaviors of sediments in contrast to the diverse characteristics of MPs. Besides, MP transport in reservoirs is more prone to the influences of anthropogenic activities (e.g., WWTP effluents) than SS transport (Balla et al., 2022). For instance, the MP concentration in the impounded section of the Kisköre Dam declined downstream simultaneously with the decrease in SSC. Sill it increased in the reservoir of the Novi Becej Dam. This unexpected increase in the reservoir of the Novi Becej Dam might be originated from the increased input from local MP sources (e.g., unmanaged wastewater, effluents from WWTPs), as this section of the Tisza is in Serbia, where wastewater management is the worst.

Watkins et al. (2019) also reported both increasing and decreasing MP concentration in reservoirs, though the decreasing trend was the most common condition. Although some patterns were identified for SS and MP in the reservoirs, these patterns are still uncertain due to the low number of sampling sites; thus denser sampling network is necessary to confirm the longitudinal SS and MP transport variations in reservoirs and downstream of them.

5.5. Validity of the suspended sediment concentration estimations based on Sentinel-2 images

The validation of the machine-learning-based SSC model applying Sentinel-2A-B images suggested that it could be employed as a reliable tool to estimate SSC, because the estimated SSC values in 2022 (mean: 40.2 ± 9.8 g/m^3) were consistent with the simultaneously measured data (mean: 38.6 ± 10.7 g/m^3), However, the limitations of the method should be kept in mind, since it overestimates the real SSC in case of intensive algae growth (in 2022: sites "w–z") or when the water is very shallow, and its bottom is visible (in 2021 and 2022: sites "a–b"). Besides, the agreement during floods was better than at low stages, probably because the low stage measurements represent summer days with more algae and busier traffic on the river, increasing the SSC along the banks by accelerated wave action.

As a strong positive correlation exists between the SS and MP concentrations in the Tisza during flood waves, rating curves could be produced for these higher stages, which could be employed to give rough estimates for the MP concentration based on SSC measured or estimated by satellite images. This offers a potentially cost-effective and efficient method for monitoring microplastic transport.

6. Conclusions

The influencing factors on SS and MP concentrations of a medium-sized, lowland river were evaluated based on frequently repeated (5 days) year-long measurements (May 2021–May 2022) at one site and two surveys along the entire 962 km-long Tisza River (Central Europe).

The water stage, SS, and MP concentrations are strongly correlated during flood waves, but the correlation is negligible during low stages. Based on the conceptual model of this study, during low stages, natural sediment sources (e.g., runoff, mobilization of in-channel sediments) are less active than anthropogenic sources (e.g., direct wastewater drainage, effluence from WWTPs), thus, there is a negligible correlation between SS and MP concentrations. As the flood waves are initiated by increased runoff, especially in the mountainous sections of the river and tributaries, more natural sediment and waste can get into the river system. Besides, the increased energy of the flood waves mobilizes the sediments (including MP) from the channel bottom. Therefore, the SS and MP concentrations are more strongly related during floods. However, the event sequence is important, as the sediments are more effectively mobilized during the rising limb of the flood waves and during the first flood wave after a long dry period. Thus, the SS and MP transport could be higher than during the falling limb of floods or during subsequent floods with a similar magnitude. It suggests that the hydrological conditions of a river should be carefully analyzed in planning the monitoring of SS and MP concentrations, as comparable results can be obtained only in the frame of hydrological background.

The repeated longitudinal measurements proved that the trend of downstream SS and MP transport is influenced by several natural (e.g., slope, flow velocity, tributaries) and anthropogenic factors (e.g., distance from the main pollutant sources, impoundment, and incision caused by dams), though the influence of tributaries and dams require further research. The SS transport is more likely to be influenced by tributaries and slope changes (including the effects of dams), while the MP transport is mainly governed by wastewater discharges. In case of rivers with artificial levee systems, the lateral transport of materials is impeded, thus SSs and MPs can get into the system via runoff just from the mountainous-hilly areas of the sub-catchments, although the MP input from WWTPs can be all along the river. This also applies to the tributaries, which can carry significant amounts of SS and MP into the main river; however, their effectivity is dependent on their discharge.

As the spatial complexity of the influencing factors is combined with the temporal changes in water and SS discharge, complex pollution patterns can develop. Thus, snapshot surveys can result in very contradictory results. Therefore, denser spatial and temporal monitoring of MP is suggested if the aim is to understand the sources, transport, and sinks of MP in a fluvial environment.

CRediT authorship contribution statement

Ahmed Mohsen: Methodology, Software, Validation, Formal analysis, Investigation, Writing – original draft, Writing – review & editing.

Alexia Balla: Validation, Investigation, Data curation, Writing – review & editing. **Tímea Kiss:** Conceptualization, Methodology, Investigation, Resources, Writing – review & editing, Supervision, Visualization, Project administration.

Declaration of competing interest

The authors declare that they have no known competing financial interests or personal relationships that could have appeared to influence the work reported in this paper.

Data availability

The data used in this research is available upon request.

Acknowledgements

The research was funded by the Hungarian Research Foundation (OTKA 134306). Ahmed Mohsen is a Ph.D. student funded by a scholarship of the Tempus Public Fundation (SHE-13402-004/2020) under the joint executive program between the Arab Republic of Egypt and Hungary. We are grateful for the ferrymen at Mindszent, who supported the pumping. We are thankful for the hydrological data provided by Hydrological Water Directorate of the Lower Tisza (ATIVIZIG), and for Dr. Vesna Teofilović (Faculty of Technology, University of Novi Sad) to support FTIR measurements.

Appendix A. Supplementary data

Supplementary data to this article can be found online at https://doi.org/10.1016/j.scitotenv.2023.166188.

References

Akyildiz, S.H., Bellopede, R., Sezgin, H., Yalcin-Enis, I., Yalcin, B., Fiore, S., 2022. Detection and analysis of microfibers and microplastics in wastewater from a textile company. Microplastics 572–586. https://doi.org/10.3390/microplastics1040040.

ASTM, 2007. Standard Test Method for Determining Sediment Concentration in Water Samples, West Conshohocken, PA. D3977-97R07. https://doi.org/10.1520/D3977-97R07.

Balla, A., Mohsen, A., Gönczy, S., Kiss, T., 2022. Spatial Variations in Microfiber Transport in a Transnational River Basin. Appl. Sci. 12 (21), 10852. https://doi.org/10.3390/app122110852.

Barrows, A.P.W., Christiansen, K.S., Bode, E.T., Hoellein, T.J., 2018. A watershed-scale, citizen science approach to quantifying microplastic concentration in a mixed land-use river. Water Res. 147, 382–392. https://doi.org/10.1016/j.watres.2018.10.013.

Bashir, S.M., Kimiko, S., Mak, C.-W., Fang, J.K.-H., Gonçalves, D., 2021. Personal care and cosmetic products as a potential source of environmental contamination by microplastics in a densely populated asian city. Front. Mar. Sci. 8 https://doi.org/10.3389/fmars.2021.683482.

Béjar, M., Vericat, D., Batalla, R.J., Gibbins, C.N., 2018. Variation in flow and suspended sediment transport in a montane river affected by hydropeaking and instream mining. Geomorphology 310, 69–83. https://doi.org/10.1016/j.geomorph.2018.03.001.

Chen, H.L., Gibbins, C.N., Selvam, S.B., Ting, K.N., 2021. Spatio-temporal variation of microplastic along a rural to urban transition in a tropical river. Environ. Pollut. 289, 117895 https://doi.org/10.1016/j.envpol.2021.117895.

Cowger, W., Gray, A.B., Guilinger, J.J., Fong, B., Waldschläger, K., 2021. Concentration depth profiles of microplastic particles in river flow and implications for surface sampling. Environ. Sci. Technol. 55 (9), 6032–6041. https://doi.org/10.1021/acs.est.1c01768.

Csépes, E., Nagy, M., Bancsi, I., Végvári, P., Kovács, P., Szilágyi, E., 2000. The phases of water quality characteristics in the middle section of river Tisza in the light of the greatest flood of the century. Hidrológiai Közlöny 80, 285–287 (in Hungarian).

Csépes, E., Bancsi, I., Végvári, P., Aranyné Rózsavári, A., 2003. Sediment transport study on the Middle Tisza (between Kisköre and Szolnok). MHT Szolnok 2 (CD), 1–10 (in Hungarian).

Dancey, C.P., Reidy, J., 2007. Statistics Without Maths for Psychology, Fourth edition. Pearson education limited, England.

Davis, B.E., 2005. A Guide to the Proper Selection and Use of Federally Approved Sediment and Water-Quality Samplers. US Department of the Interior, US Geological Survey.

Eurostat, 2021. Municipal waste statistics. https://ec.europa.eu/eurostat/statistics-explained/index.php?title=Municipal_waste_statistics (Accessed on February 6th, 2022).

Feng, S., Lu, H., Tian, P., Xue, Y., Lu, J., Tang, M., Feng, W., 2020. Analysis of microplastics in a remote region of the Tibetan Plateau: Implications for natural environmental response to human activities. Sci. Total Environ. 739, 140087 https://doi.org/10.1016/j.scitotenv.2020.140087.

Grbić, J., Helm, P., Athey, S., Rochman, C.M., 2020. Microplastics entering northwestern Lake Ontario are diverse and linked to urban sources. Water Res. 174, 115623 https://doi.org/10.1016/j.watres.2020.115623.

Grove, M.K., Bilotta, G.S., Woockman, R.R., Schwartz, J.S., 2015. SS regimes in contrasting reference-condition freshwater ecosystems: implications for water quality guidelines and management. Sci. Total Environ. 502, 481–492. https://doi.org/10.1016/j.scitotenv.2014.09.054.

He, P., Chen, L., Shao, L., Zhang, H., Lü, F., 2019. Municipal solid waste (MSW) landfill: a source of microplastics? -Evidence of microplastics in landfill leachate. Water Res. 159, 38–45. https://doi.org/10.1016/j.watres.2019.04.060.

He, D., Chen, X., Zhao, W., Zhu, Z., Qi, X., Zhou, L., Chen, W., Wan, C., Li, D., Zou, X., Wu, N., 2021. Microplastics contamination in the surface water of the Yangtze River from upstream to estuary based on different sampling methods. Environ. Res. 196, 110908 https://doi.org/10.1016/j.envres.2021.110908.

Hurley, R., Woodward, J., Rothwell, J.J., 2018. Microplastic contamination of river beds significantly reduced by catchment-wide flooding. Nat. Geosci. 11 (4), 251–257. https://doi.org/10.1038/s41561-018-0080-1.

ICPDR, 2018. Tisza River Basin Characterization Report on Surface Water, Interreg (Danube Transational Programme). https://www.interreg-danube.eu/uploads/media/approved_project_output/0001/37/ed1b7198ffc57c6d2d528717650cd6d94280004e.pdf (Accessed on May 15th, 2022).

Interreg, 2018. Report on significant pressures relevant for the Tisza River Basin. Deliverable 3.2.1 Report on significant pressures relevant for the TRB, Danube Transnational Programme. https://www.interreg-danube.eu/approved-projects/jointisza (Accessed on May 15th, 2022).

Karimaee Tabarestani, M., Zarrati, A.R., 2015. Sediment transport during flood event: a review. Int. J. Environ. Sci. Technol. 12 (2), 775–788. https://doi.org/10.1007/s13762-014-0689-6.

Kiss, T., Fiala, K., Sipos, G., 2008. Alterations of channel parameters in response to river regulation works since 1840 on the Lower Tisza River (Hungary). Geomorphology 98 (1), 96–110. https://doi.org/10.1016/j.geomorph.2007.02.027.

Kiss, T., Fiala, K., Sipos, G., Szatmári, G., 2019. Long-term hydrological changes after various river regulation measures: are we responsible for flow extremes? Hydrol. Res. 50 (2), 417–430. https://doi.org/10.2166/nh.2019.095.

Kiss, T., Fórián, S., Szatmári, G., Sipos, G., 2021. Spatial distribution of microplastics in the fluvial sediments of a transboundary river – a case study of the Tisza River in Central Europe. Sci. Total Environ. 785, 147306 https://doi.org/10.1016/j.scitotenv.2021.147306.

Kiss, T., Gönczy, S., Nagy, T., Mesaroš, M., Balla, A., 2022. Deposition and mobilization of microplastics in a low-energy fluvial environment from a geomorphological perspective. Appl. Sci. 12 (9), 4367. https://doi.org/10.3390/app12094367.

Kondolf, G.M., Gao, Y., Annandale, G.W., Morris, G.L., Jiang, E., Zhang, J., Cao, Y., Carling, P., Fu, K., Guo, Q., Hotchkiss, R., Peteuil, C., Sumi, T., Wang, H.-W., Wang, Z., Wei, Z., Wu, B., Wu, C., Yang, C.T., 2014. Sustainable sediment management in reservoirs and regulated rivers: Experiences from five continents. Earth's Future 2 (5), 256–280. https://doi.org/10.1002/2013EF000184.

Koyuncuoğlu, P., Erden, G., 2023. Microplastics in municipal wastewater treatment plants: a case study of Denizli/Turkey. Front. Environ. Sci. Eng. 17 (8), 99. https://doi.org/10.1007/s11783-023-1699-8.

Kruskal, W.H., Wallis, W.A., 1952. Use of ranks in one-criterion variance analysis. J. Am. Stat. Assoc. 47 (260), 583–621. https://doi.org/10.1080/01621459.1952.10483441.

Laermanns, H., Reifferscheid, G., Kruse, J., Földi, C., Dierkes, G., Schaefer, D., Scherer, C., Bogner, C., Stock, F., 2021. Microplastic in water and sediments at the confluence of the Elbe and Mulde Rivers in Germany. Front. Environ. Sci. 9, 794895 https://doi.org/10.3389/fenvs.2021.794895.

Lászlóffy, W., 1982. Tisza river: construction and water management in the Tisza water regime (title translated from Hungarian). Akadémiai Kiadó, Budapest, Hungary.

Matjašič, T., Mori, N., Hostnik, I., Bajt, O., Kovač Viršek, M., 2023. Microplastic pollution in small rivers along rural–urban gradients: Variations across catchments and between water column and sediments. Sci. Total Environ. 858, 160043 https://doi.org/10.1016/j.scitotenv.2022.160043.

Mattos, L.D., Kruger, L.D.M., Affonso, A.L.S., Perbiche-Neves, G., Pressinatte, S., 2017. Small dams also change the benthic macroinvertebrates community in rocky rivers. Acta Limnol. Bras. 29 https://doi.org/10.1590/s2179-975x5316.

McFeeters, S.K., 1996. The use of the Normalized Difference Water Index (NDWI) in the delineation of open water features. Int. J. Remote Sens. 17 (7), 1425–1432. https://doi.org/10.1080/01431169608948714.

Mihai, F.-C., Gündoğdu, S., Markley, L.A., Olivelli, A., Khan, F.R., Gwinnett, C., Gutberlet, J., Reyna-Bensusan, N., Llanquileo-Melgarejo, P., Meidiana, C., Elagroudy, S., Ishchenko, V., Penney, S., Lenkiewicz, Z., Molinos-Senante, M., 2022. Plastic pollution, waste management issues, and circular economy opportunities in rural communities. Sustainability 14 (1). https://doi.org/10.3390/su14010020.

Mohsen, A., Kovács, F., Kiss, T., 2022. Remote sensing of sediment discharge in rivers using sentinel-2 images and machine-learning algorithms. Hydrology 9 (5), 88. https://doi.org/10.3390/hydrology9050088.

Mouri, G., Ros, F.C., Chalov, S., 2014. Characteristics of suspended sediment and river discharge during the beginning of snowmelt in volcanically active mountainous environments. Geomorphology 213, 266–276. https://doi.org/10.1016/j.geomorph.2014.02.001.

Napper, I.E., Baroth, A., Barrett, A.C., Bhola, S., Chowdhury, G.W., Davies, B.F.R., Duncan, E.M., Kumar, S., Nelms, S.E., Hasan Niloy, M.N., Nishat, B., Maddalene, T., Thompson, R.C., Koldewey, H., 2021. The abundance and characteristics of

microplastics in surface water in the transboundary Ganges River. Environ. Pollut. 274, 116348 https://doi.org/10.1016/j.envpol.2020.116348.
Ngo, P.L., Pramanik, B.K., Shah, K., Roychand, R., 2019. Pathway, classification and removal efficiency of microplastics in wastewater treatment plants. Environ. Pollut. 255, 113326 https://doi.org/10.1016/j.envpol.2019.113326.
Ockelford, A., Cundy, A., Ebdon, J.E., 2020. Storm response of fluvial sedimentary microplastics. Sci. Rep. 10 (1), 1865. https://doi.org/10.1038/s41598-020-58,765-2.
Otsu, N., 1979. A threshold selection method from gray-level histograms. IEEE Trans. Syst. Man Cybern. 9 (1), 62–66. https://doi.org/10.1109/TSMC.1979.4310076.
Overstreet, B.T., Legleiter, C.J., 2017. Removing sun glint from optical remote sensing images of shallow rivers. Earth Surf. Process. Landf. 42 (2), 318–333. https://doi.org/10.1002/esp.4063.
OVF, 2019. Yearbook (2016) of the Hydrographical Service of Hungary, 350. OVF, Budapest.
Piehl, S., Atwood, E.C., Bochow, M., Imhof, H.K., Franke, J., Siegert, F., Laforsch, C., 2020. Can water constituents be used as proxy to map microplastic dispersal within transitional and coastal waters? Front. Environ. Sci. 8, 92. https://doi.org/10.3389/fenvs.2020.00092.
Rodrigues, S.M., Almeida, C.M.R., Silva, D., Cunha, J., Antunes, C., Freitas, V., Ramos, S., 2019. Microplastic contamination in an urban estuary: abundance and distribution of microplastics and fish larvae in the Douro estuary. Sci. Total Environ. 659, 1071–1081. https://doi.org/10.1016/j.scitotenv.2018.12.273.
Rodrigues, M.O., Gonçalves, A.M.M., Gonçalves, F.J.M., Abrantes, N., 2020. Improving cost-efficiency for MPs density separation by zinc chloride reuse. MethodsX 7, 100785. https://doi.org/10.1016/j.mex.2020.100785.
Ronkay, F., Molnar, B., Gere, D., Czigany, T., 2021. Plastic waste from marine environment: demonstration of possible routes for recycling by different manufacturing technologies. Waste Manag. 119, 101–110. https://doi.org/10.1016/j.wasman.2020.09.029.
Sang, W., Chen, Z., Mei, L., Hao, S., Zhan, C., Zhang, W.B., Li, M., Liu, J., 2021. The abundance and characteristics of microplastics in rainwater pipelines in Wuhan. China. Science of the total environment 755, 142606. https://doi.org/10.1016/j.scitotenv.2020.142606.
Scherer, C., Weber, A., Stock, F., Vurusic, S., Egerci, H., Kochleus, C., Arendt, N., Foeldi, C., Dierkes, G., Wagner, M., Brennholt, N., Reifferscheid, G., 2020. Comparative assessment of microplastics in water and sediment of a large European river. Sci. Total Environ. 738, 139866 https://doi.org/10.1016/j.scitotenv.2020.139866.
Schrank, I., Löder, M.G.J., Imhof, H.K., Moses, S.R., Heß, M., Schwaiger, J., Laforsch, C., 2022. Riverine microplastic contamination in southwest Germany: a large-scale survey. Front. Earth Sci. 10, 794250 https://doi.org/10.3389/feart.2022.794250.
Serra, T., Soler, M., Barcelona, A., Colomer, J., 2022. Suspended sediment transport and deposition in sediment-replenished artificial floods in Mediterranean rivers. J. Hydrol. 609, 127756 https://doi.org/10.1016/j.jhydrol.2022.127756.
Talbot, R., Chang, H., 2022. Microplastics in freshwater: a global review of factors affecting spatial and temporal variations. Environ. Pollut. 292, 118393 https://doi.org/10.1016/j.envpol.2021.118393.
Tamminga, M., Stoewer, S.-C., Fischer, E.K., 2019. On the representativeness of pump water samples versus manta sampling in microplastic analysis. Environ. Pollut. 254, 112970 https://doi.org/10.1016/j.envpol.2019.112970.
Tang, K.H.D., Hadibarata, T., 2021. Microplastics removal through water treatment plants: Its feasibility, efficiency, future prospects and enhancement by proper waste management. Environ. Chall. 5, 100264 https://doi.org/10.1016/j.envc.2021.100264.
Tarpai, J., 2013. The Role of Natural and Social Resources in the Touristical Development of the Transcarpathian Region, Ukraine. PhD Thesis,. University of Pécs.
Tibbetts, J., Krause, S., Lynch, I., Sambrook Smith, G.H., 2018. Abundance, distribution, and drivers of microplastic contamination in urban river environments. Water 10 (11). https://doi.org/10.3390/w10111597.
Vercruysse, K., Grabowski, R.C., Rickson, R., 2017. Suspended sediment transport dynamics in rivers: Multi-scale drivers of temporal variation. Earth Sci. Rev. 166, 38–52.
Waldschläger, K., Schüttrumpf, H., 2019. Effects of particle properties on the settling and rise velocities of microplastics in freshwater under laboratory conditions. Environ. Sci. Technol. 53 (4), 1958–1966. https://doi.org/10.1021/acs.est.8b06794.
Wang, Q., Huang, K., Li, Y., Zhang, Y., Yan, L., Xu, K., Huang, S., Junaid, M., Wang, J., 2022. Microplastics abundance, distribution, and composition in freshwater and sediments from the largest Xijin Wetland Park, Nanning, South China. Gondwana Res. 108, 13–21. https://doi.org/10.1016/j.gr.2021.07.009.
Watkins, L., McGrattan, S., Sullivan, P.J., Walter, M.T., 2019. The effect of dams on river transport of microplastic pollution. Sci. Total Environ. 664, 834–840. https://doi.org/10.1016/j.scitotenv.2019.02.028.
Wu, P., Tang, Y., Dang, M., Wang, S., Jin, H., Liu, Y., Jing, H., Zheng, C., Yi, S., Cai, Z., 2020. Spatial-temporal distribution of microplastics in surface water and sediments of Maozhou River within Guangdong-Hong Kong-Macao Greater Bay Area. Sci. Total Environ. 717, 135187 https://doi.org/10.1016/j.scitotenv.2019.135187.
Yan, Z., Chen, Y., Bao, X., Zhang, X., Ling, X., Lu, G., Liu, J., Nie, Y., 2021. Microplastic pollution in an urbanized river affected by water diversion: Combining with active biomonitoring. J. Hazard. Mater. 417, 126058 https://doi.org/10.1016/j.jhazmat.2021.126058.
Yuan, X., Tian, F., Wang, X., Liu, Y., Chen, M.-T., 2018. Small-scale sediment scouring and siltation laws in the evolution trends of fluvial facies in the Ningxia Plain Reaches of the Yellow River (NPRYR). Quat. Int. 476, 14–25. https://doi.org/10.1016/j.quaint.2018.03.034.
Zhang, L., Liu, J., Xie, Y., Zhong, S., Yang, B., Lu, D., Zhong, Q., 2020. Distribution of microplastics in surface water and sediments of Qin river in Beibu Gulf, China. Sci. Total Environ. 708, 135176 https://doi.org/10.1016/j.scitotenv.2019.135176.